ISBN: 978-3-95450-231-8 ISSN: 2673-5490 doi: 10.18429/JACoW-IPAC2023-WEPL078

ANALYZING AND OPTIMIZING DYNAMIC APERTURE BASED ON MINIMIZING THE FLUCTUATION OF RESONANCE DRIVING TERMS

Bingfeng Wei, Jiajie Tan, Zhenghe Bai*, Guangyao Feng†
National Synchrotron Radiation Laboratory, USTC, Hefei, China

Abstract

Minimizing resonance driving terms (RDTs) is a traditional approach to enlarge the dynamic aperture (DA) of a storage ring. However, small RDTs can not guarantee a large DA. In this paper, the fluctuation of RDTs along the ring is taken into consideration. A large number of nonlinear lattice solutions based on one double-bend achromat lattice are analyzed. The results show that minimizing the RDT fluctuations can more effectively enlarge the DA area than minimizing the commonly used one-turn RDTs. Also, reducing the third-order RDT fluctuations is beneficial for controlling the fourth-order RDTs and ADTS terms. Then, we use it as an objective to optimize the nonlinear dynamics and good results are obtained.

INTRODUCTION

Dynamic aperture (DA) is one of the most important properties of a storage ring. Minimizing the resonance driving terms (RDTs) is a traditional analytical approach for DA optimization [1]. In this analytical approach, minimizing RDTs to suppress the corresponding resonances and also controlling amplitude dependent tune shifts (ADTS) to avoid resonance crossings can help to enlarge the DA. However, small RDTs is a necessary but not sufficient condition for large DA [2].

The local cancellation of nonlinear effects, which has been applied to some diffraction-limited storage ring lattices, prevents the RDTs from building up along the ring and is more effective than the global cancellation [3]. Moreover, minimizing the turn-by-turn fluctuations of Courant-Snyder actions of particles helps to enlarge the DA [4]. The fluctuation of Courant-Snyder actions is related to the fluctuation of RDTs. These inspire us the importance of suppressing the building up of RDTs. In this paper, the RDTs will be calculated as functions of position to demonstrate their fluctuations along the ring. We will analyze the correlation between the DA area and RDT fluctuations using a double-bend achromat (DBA) lattice as an example. Then, we will optimize the nonlinear dynamics of the DBA lattice by minimizing the RDT fluctuations.

DA ANALYSIS BASED ON MINIMIZING RDT FLUCTUATIONS

Here, we use the SSRF storage ring lattice for the DA analysis. SSRF is a third-generation synchrotron light source with a beam energy of 3.5 GeV and a natural emittance

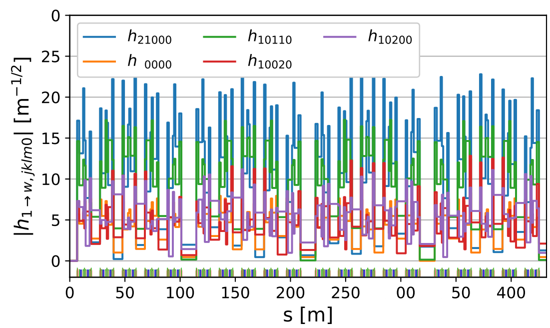

Figure 1: Fluctuation of the third-order geometric RDTs of the SSRF storage ring lattice.

of 3.9 nm·rad [5]. The storage ring consists of 4 superperiods, each containing 5 DBA cells. There are 2 chromatic sextupole families and 6 harmonic sextupole families.

Each sextupole is a nonlinear kick, which perturbs the linear motion of particles. The perturbation of the i-th sextupole in the normal form is denoted as $\hat{V}_i$. They contribute to the third-order generator for the ring Hamiltonian as $h_3 = \sum_{i=1}^{N} \hat{V}_i$, where N is the number of sextupoles of the ring. The crossing terms of two sextupoles contribute to the fourth-order generator as

$$h_4 = \sum_{j>i=1}^{N} \left[\hat{V}_i, \hat{V}_j\right] = \sum_{j=2}^{N} \left[\sum_{i=1}^{j-1} \hat{V}_i, \hat{V}_j\right]. \qquad (1)$$

The increment of the fourth-order RDTs at the j-th sextupole can be considered as the Poisson bracket of the perturbation accumulated before it and generated by it. Reducing the accumulated perturbations, i.e. the third-order RDT fluctuations, can be beneficial for controlling the fourth-order RDTs. Additionally, if we record the third-order RDT fluctuations, we can directly obtain the values of $\sum_{i=1}^{j-1} \hat{V}_i$ in Eq. (1), reducing the calculation to a single loop and greatly increasing the calculation speed.

The generators can be expanded by the resonance basis to obtain the RDTs h_{jklmp}. We can also expand $\sum_{i=1}^{w} \hat{V}_i$ and $\sum_{j>i=1}^{w} \left[\hat{V}_i, \hat{V}_j\right]$ with the resonance basis to show the RDTs accumulated from the first sextupole to the w-th sextupole, denoted as $h_{1\to w,jklmp}$. Then, $h_{1\to w,jklmp}$ with different w show the RDT fluctuations. Figure 1 shows the fluctuation of the third-order geometric RDTs of the SSRF storage ring lattice. They change at the locations of sextupoles (green blocks at the bottom). The one-turn value, i.e. the geometric RDTs of the one-turn map, is denoted as $h_{jklm0,\mathrm{ring}}$, where the subscript $p = 0$ for geometric terms. In addition, we will control the average value of the geometric RDTs at all locations of sextupoles along the ring, denoted as $h_{jklm0,\mathrm{ave}}$, i.e.

* baizhe@ustc.edu.cn
† fenggy@ustc.edu.cn

© Content from this work may be used under the terms of the CC BY 4.0 licence (© 2022). Any distribution of this work must maintain attribution to the author(s), title of the work, publisher, and DOI.
This is a preprint - the final version is published with IOP

ISBN: 978-3-95450-231-8 ISSN: 2673-5490 doi: 10.18429/JACoW-IPAC2023-WEPL078

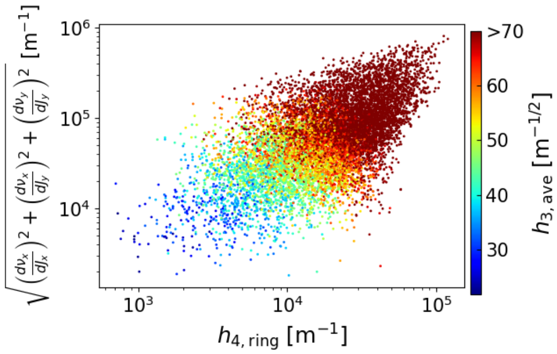

Figure 2: Correlation between the third-order RDT fluctuations $h_{3,\mathrm{ave}}$, the fourth-order one-turn RDTs $h_{4,\mathrm{ring}}$ and the ADTS terms. The latter two represented by the axes are contributed by sextupole crossing terms. The color bar shows the value of $h_{3,\mathrm{ave}}$.

$\sum_{i=1}^{N} \left|h_{1\to i,jklm0}\right| / N \equiv h_{jklm0,\mathrm{ave}}$. Different RDTs driving different resonances are not of the same importance. It is complicated to consider them separately. For simplicity, the RDTs of the same order have the same weight in this paper. Then, the fluctuation of the n-th order RDTs is calculated as

$$h_{n,\mathrm{ave}} = \sqrt{\sum_{j+k+l+m=n} (h_{jklm0,\mathrm{ave}})^2} \tag{2}$$

and the n-th order one-turn RDTs $h_{n,\mathrm{ring}}$ is defined in the same way.

To analyze the correlation between the third-order RDT fluctuations and the crossing terms, we generated 10000 random nonlinear solutions with horizontal and vertical chromaticities corrected to $(1, 1)$. Both the fourth-order RDTs and the ADTS terms are generated by the sextupole crossing terms. The correlation between them and the third-order RDT fluctuations is shown in Fig. 2. As the third-order RDT fluctuations reduce, both the fourth-order RDTs and the ADTS terms also roughly reduce. So reducing the third-order RDT fluctuations can effectively control the fourth-order RDTs and ADTS terms.

Next, we step further to analyze the correlation between the RDT fluctuations and DA area. Because the possibility of a random nonlinear solution having a large DA is very small, we minimized the third-order one-turn RDTs with a genetic algorithm toolbox geatpy [6] to obtain more solutions with large DAs. The strengths of 6 harmonic sextupole families were variables, and the 2 chromatic sextupole families were used to fix the corrected chromaticities to (1, 1). After 40 generations with a population size of 10000, the $h_{3,\mathrm{ring}}$ of the population were optimized to small values. And the third-order RDTs of some solutions are almost completely cancelled. Then, we used the solutions with small ADTS terms for further analysis. The on-momentum DA areas of these solutions were calculated with ELEGANT [7].

The correlation between $h_{3,\mathrm{ring}}$, $h_{3,\mathrm{ave}}$ and the DA area is shown in Fig. 3. In Fig. 3(a), following [2], we use the two axes to represent the one-turn RDTs and the DA area.

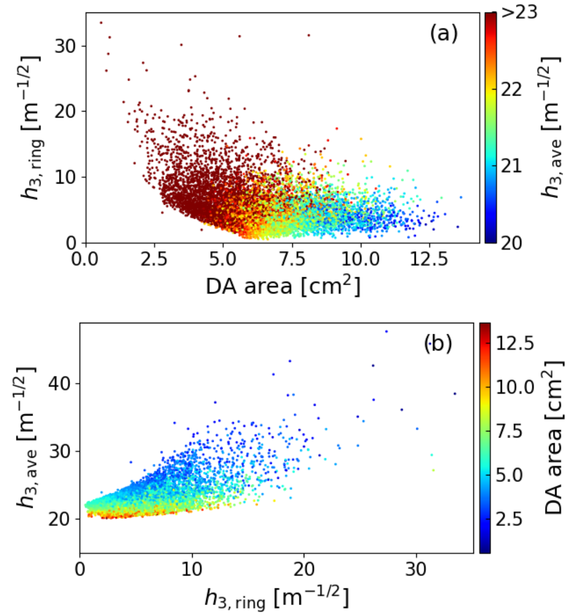

Figure 3: Correlation between the RDT fluctuations, the one-turn RDTs and the DA area for the SSRF storage ring lattice. The solutions were obtained after the optimization using a genetic algorithm toolbox geatpy.

Besides, a color bar is added to show the RDT fluctuations. We see that small RDTs is a necessary but not sufficient condition for large DA, which is consistent with [2]. However, $h_{3,\mathrm{ave}}$ shows a stronger correlation with the DA area. In Fig. 3(b), we change the axes to represent $h_{3,\mathrm{ring}}$ and $h_{3,\mathrm{ave}}$, while the color bar shows the DA area. The colors are roughly layered, and the red dots with large DAs sink to the bottom. The distribution once again indicates that minimizing $h_{3,\mathrm{ave}}$ is more effective than minimizing $h_{3,\mathrm{ring}}$ to enlarge the DA. Also, it can be seen that when $h_{3,\mathrm{ave}}$ is minimized, the one-turn RDTs $h_{3,\mathrm{ring}}$ is also controlled.

DA OPTIMIZATION BASED ON MINIMIZING RDT FLUCTUATIONS

Given the strong correlation between minimizing the RDT fluctuations and enlarging the DA area found in the previous section, we can use the former as a direct objective in the nonlinear optimization. We performed a single-objective optimization with the goal of minimizing $h_{3,\mathrm{ave}}$. The ADTS terms are not objectives, as we have verified that reducing $h_{3,\mathrm{ave}}$ can effectively control the ADTS terms in the SSRF lattice. They will be considered when selecting the optimized solutions. Other optimization settings are the same as before. The h_{ave} and h_{ring} values for the 10th, 20th, 30th and 40th generations are plotted in Fig. 4. Compared to Fig. 3(b), the results converge to a small region where large DA solutions are distributed. We randomly selected 20 solutions from the 40th generation and calculated their DA areas, all of which exceed 12.99 cm^2 with an average value of 13.39 cm^2. Therefore the fluctuation of RDTs is an effective

This is a preprint - the final version is published with IOP
Content from this work may be used under the terms of the CC BY 4.0 licence (© 2022). Any distribution of this work must maintain attribution to the author(s), title of the work, publisher, and DOI.

ISBN: 978-3-95450-231-8 ISSN: 2673-5490 doi: 10.18429/JACoW-IPAC2023-WEPL078

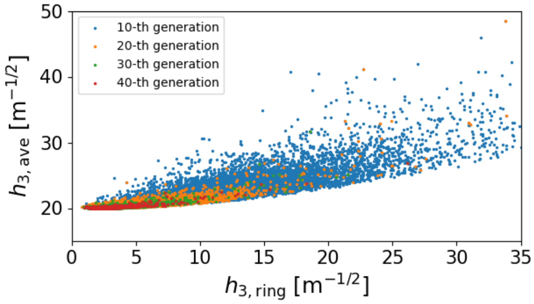

Figure 4: In the optimization of minimizing $h_{3,\mathrm{ave}}$, the results converge to a small region, which corresponds to the region with larger DA solutions distributed in Fig. 3.

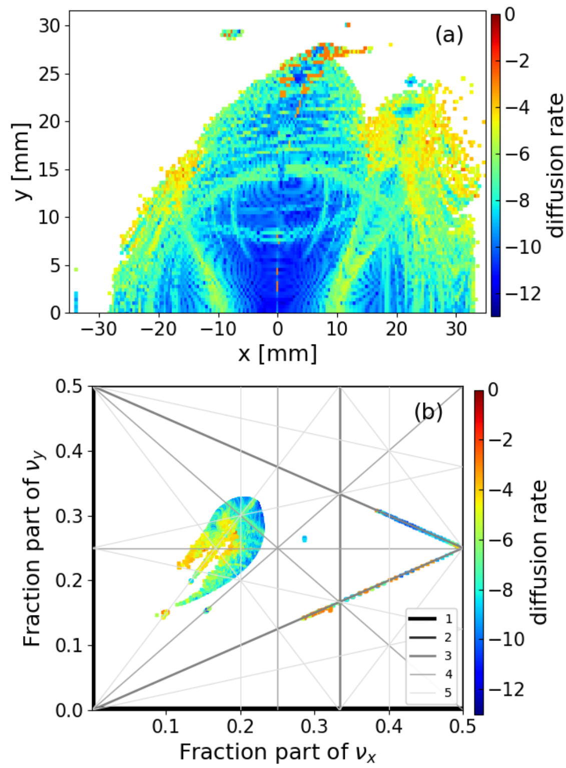

Figure 5: DA and FMA of an optimized nonlinear solution.

indicator in the nonlinear optimization, and can successfully find nonlinear solutions with large DAs.

Then, we took the ADTS terms and higher-order chromaticities into consideration, and selected a nonlinear solution from the good ones. The tracked DA and FMA results are shown in Fig. 5.

The DA is large and avoids third-order resonances as well as the majority of fourth-order resonances. In addition, we also checked the off-momentum dynamics. The off-momentum DAs and tune shifts with momentum are shown in Fig. 6. For the relative momentum deviation $\delta = \pm 3\%$, the DAs are also large, with > 24 mm in the horizontal plane. The tune shifts are well controlled, and there is no crossing between the two curves in Fig. 6(b).

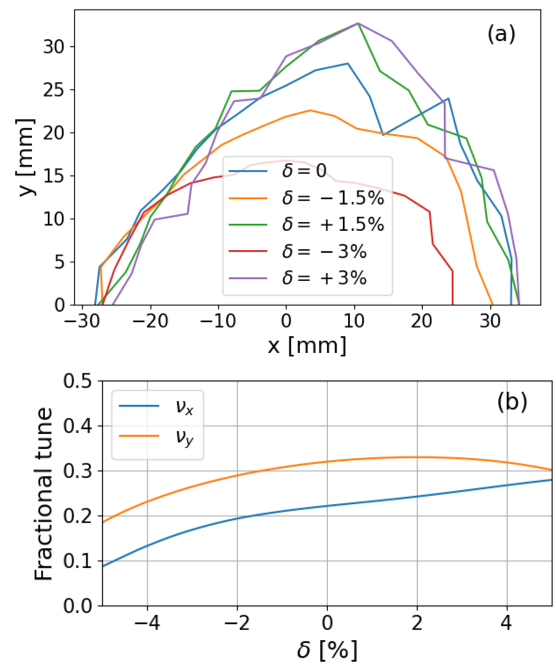

Figure 6: On- and off-momentum DAs (a) and tune shifts with momentum (b) of the optimized solution. The δ is the relative momentum deviation.

CONCLUSION

The correlation between the RDT fluctuations, the one-turn RDTs and the DA area of one DBA lattice was analyzed in this paper. It was found that reducing the third-order RDT fluctuations can effectively reduce crossing terms, such as the fourth-order RDTs and ADTS terms. Furthermore, a significant correlation was found between large DA area and small RDT fluctuations. Based on these findings, we minimized RDT fluctuations to optimize the DA of the lattice, and obtained numerous solutions with large DAs. For a more complicated lattice, the ADTS terms, higher-order chromaticities, chromatic RDTs fluctuations and higher-order RDTs as well as their fluctuations could be also considered as objectives to perform a more comprehensive optimization. And particle tracking can be used to further optimize the DA once the region with good solutions is found. The code for faster calculation of the fourth-order RDTs and for calculating the RDT fluctuations has been shared on a GitHub page [8].

ACKNOWLEDGEMENTS

This work was supported by the National Natural Science Foundation of China under Grant No. 11875259.

REFERENCES

[1] J. Bengtsson, "The Sextupole Scheme for the Swiss Light Source (SLS): An Analytic Approch", PSI, Villigen, Switzerland, SLS Note 9/97, 1997.

[2] L. Yang, Y. Li, W. Guo, and S. Krinsky, "Multiobjective optimization of dynamic aperture", *Phys. Rev. Spec. Top. Accel*

Content from this work may be used under the terms of the CC BY 4.0 licence (© 2022). Any distribution of this work must maintain attribution to the author(s), title of the work, publisher, and DOI.

This is a preprint - the final version is published with IOP

ISBN: 978-3-95450-231-8 ISSN: 2673-5490 doi: 10.18429/JACoW-IPAC2023-WEPL078

Beams, vol. 14, p. 054001, 2011. doi:10.1103/PhysRevSTAB.14.054001

[3] R. Bartolini, "Storage Ring Design for Synchrotron Radiation Sources", in *Synchrotron Light Sources and Free-Electron Lasers*, Switzerland: Springer, Cham, 2020, pp. 273–322. doi:10.1007/978-3-319-04507-8

[4] Y. Li, K. Hwang, C. Mitchell, R. Rainer, R. Ryne, and V. Smaluk, "Design of double-bend and multibend achromat lattices with large dynamic aperture and approximate invariants", *Phys. Rev. Accel. Beams*, vol. 24, p. 124001, 2021. doi:10.1103/PhysRevAccelBeams.24.124001

[5] G. Liu *et al.*, "Lattice design for SSRF storage ring", *High Energy Phys. and Nucl. Phys.*, vol. 30, pp. 144–146, 2006.

[6] Jazzbin *et al.*, "geatpy: The genetic and evolutionary algorithm toolbox with high performance in python", 2020, http://www.geatpy.com/.

[7] M. Borland, "elegant: A Flexible SDDS-Compliant Code for Accelerator Simulation", ANL, IL, USA, LS-287, Sep. 2000. doi:10.2172/761286

[8] Simple storage ring, https://github.com/wei0852/simplestoragering

Content from this work may be used under the terms of the CC BY 4.0 licence (© 2022). Any distribution of this work must maintain attribution to the author(s), title of the work, publisher, and DOI.

This is a preprint - the final version is published with IOP